An Experimental Investigation of the Influence of Point Angle and Fluctuation in Thrust Force On Chip Morphology

Zulkuf Demir
Batman University, Mechanical Engineering, Batman/Turkey

ABSTRACT

Drilling is a widely used machining method in engineering applications, playing a major part in machining operations. Chip morphology is an indicator, which shows the quality of machining. Especially, chip thickness ratio is a characteristic to show the level of deformation and cutting effects during machining operations. In the present paper, the influences of parameters such as feed rate, spindle speed, point angle, and fluctuation size on the chip morphology investigated. The most influential parameter on the chip thickness was feed rate, while point angle on the chip width. The most favourable chip thickness ratio values and a lower fluctuation size in thrust force were achieved at 100° and 118° point angles. Although the higher fluctuation in thrust force and chip thickness ratio values were observed at 136° and 154° point angles, the most favourable chip morphology was obtained at these point angles. In other words, the higher point angles were found to be advantages in drilling operations to obtain a better chip morphology and chip geometrical dimensions.

Keywords:
Drilling; Point angle; Chip thickness; Chip morphology; Chip width.

INTRODUCTION

Drilling is a machining method, improving attractive geometric and dimensional precision in manufacturing operations [1]. Among the conventional metal cutting manufacturing methods, drilling is one of the significant operation, playing a part approximately 33 % in metal machining [2]. Most of the researches are done using drilling manufacturing method to complexity of manufacturing process and application in a very large variety in drilling operations [3]. Many factors influence the drilling process like point angle of drill, the materials of drill and specimen. The tool materials affect the precision of the hole, by the impressions of wear of the drill, surface roughness [4].

Chip formation is a complex process with including both elastic and plastic deformations shapes [5]. These shapes reflect the behaviour of the breaking of the material as three kinds of chips in continuous, adherent, and discontinuous forms. Continuous chip can be achieved when the ductile materials are machined at low feed rates and high spindles speeds, while adherent chip taken place at medium spindle speeds. Moreover, at larger feed rates and smaller point angles chip obtain in brittle and short forms, relative to the increasing in the hardness [6, 7]. In other words, the continuous chip forms, which indicates the better results, are obtained at low cutting conditions, while the more undesired chip forms are obtained at extreme drilling conditions [8, 9]. A composite of chip dimensions commonly points out that two cutting edges angles and their lengths on both side are different. At higher cutting speeds, helix and long ribbon chip form are achieved, while at higher feed rates only long ribbon chips can be gained. This points out that stringent wear on drill taken place at higher feed rates. The loose helix chips cause to little wear on the tool [10]. Furthermore, at smaller spindle speeds short break-up chips come into existence because of the non-continuous distortion in the shear plane. At average spindle speeds provided obtaining the long helical chips. Increasing point angle causes to rise the dimension of the arc of the broken chips. At higher spindle speeds, the continuous chip achieves, while on-shaped discontinuous chip form obtains at lower spindle speed [11].

In machining operations, feed rate causes to inc-

rease pressure on the tool, which leads workpiece to plastic deformation. Lower chip thickness ratio causes to larger grade of shear plane angle, in turn induces low shear stress in the chip and decrease the using up necessary of energy. The plastic deformation region becomes smaller at larger cutting speeds. the chip thickness ratio decreases in with increasing the cutting speed in machining operations [12]. Cutting forces have a major influence on the procedure grade in machining fabricating methods. High cutting forces cause to change the shape of tool and workpiece. Naturally, thrust force increases at high feed rates due to increase the pressure load on the drill, but this pressure decreases with increasing spindle speed [13].

Thrust force and torque in drilling operations are generally carried out by the cutting and chisel edges of the drill. Most of the thrust force and torque are on the cutting edge due to the cutting action. Since the drill radius on the cutting edge is bigger than the radius on the chisel edge. The orientation of the cutting lip causes the specific cutting pressure, which has a sudden change on the efficiency of the cutting. Consequently, the point angle of the tool has a major impact on thrust force values, namely thrust force fluctuation size during the drilling process. Additionally, dispersion of cutting forces on the cutting edge effected by the radius of the drill, workpiece microstructure, and selected conditions, such as spindle speed, feed rate, cutting depth, and tool geometry [3, 14 - 16]. With optimization in results provides a diminution in thrust force and torque of around 40 % [17]. Increasing the point angle cuts down the axial impact on the workpiece and thus lower thrust forces can be achieved at lower spindle speeds. The cutting force especially thrust force in drilling process, brings about tool wear. The increase in point angle produces smaller thrust force at higher spindle speeds [9, 11, 18]. The variation in thrust force can be related to the size of the tool side. The dimension of the tool edge changes at alteration of point angles [19 - 21].

The dissimilarity in the thrust force throughout the drilling operation can be ascribed to the regional alteration in layer thickness of the laminate and the existence of the fore-cracks in the territory of the chisel edge [22, 23]. Cutting forces are essentially depended on the mechanical characteristic of the machined material, process conditions, and tool geometrical construction. When the chisel edge start penetrating in to the workpiece in the first stage thrust force reaches the maximum value until the second edge involves in cutting. The magnitude and varying inclinations in thrust force occurs at the beginning of the operation. Then the thrust force stabilizes for a while and a small alteration in the thrust force may ascribe to little geometric distinctions on the tool cutting sizes. A periodic variation containing an abruptly decrease and gradually raise in thrust force can be attributed to the cutting fluctuation of the saw-teeth

structure [24, 25].

The major point of this experimental study is to examine the impact of feed rate, spindle speed and especially point angle of the tip of the drill, on chip thickness, chip width, chip thickness ratio and chip morphology. Furthermore, the investigation of the effect of the fluctuation size in thrust force on the chip geometrical dimensions and chip morphology is another important aim of this experimental research paper.

MATERIALS AND METHODS

Experiments were realized on MEXUS 510 C-II Model Mazak Vertical Centre CNC Milling, as demonstrated in Fig. 1 (a). The AISI 1050 alloy workpieces were preliminary setup in sizes of 100x100x15 mm^3. The holes were pre-drilled 5 mm in diameter as guiding eye. The space between the centres of the holes were arranged 20 mm. The foremost hole centre was calibrated 10 mm from the corners of the sample.

Figure 1. Experimental Setup (a) MAZAK Vertical Centre NEXUS 510 C-II Model Milling Machine and Dynamometer Apparatus, (b) Kistler Type 5233 A Model Data Logger, (c) Computer.

The forces in three directions were measured in Newton unit, by using Kistler 5233A Control Unit of the dynamometer, during drilling processes, as shown in Fig. 1 (a). With the help of data logger of dynamometer as seen in Fig. 1 (b), force data were collected and recorded via a computer, as observed in Fig. 1 (c). Moreover, data was recorded on computer by using specific software, belongs to the Control Units, and data logger. Since the thrust forces in the Z direction are considerably greater than the radial and tangential forces, only the thrust force values are taken into account. Furthermore, workpieces were pre-drilled 5 mm in diameter and 13 mm in depth, in case of cutting liquid using at 1600 rpm spindle speed and 0.1 mm/rev feed rate. After holes were pre-drilled as guiding eyes, they were drilled 10 mm

Table 1. Processing conditions.

Spindle speeds	n_1=800, n_2=1200, n_3=1600 rpm
Feed rates	f_1=0.025, f_2=0.050, f_1=0.075 mm/rev
Point angles	Φ_1=100°, Φ_2=118°, Φ_3=136°, Φ_4=154°

in depth from the top surface of the workpieces in conditions, as demonstrated in Table 1.

The impact of the point angle on the outcomes studied in performed operations. For this reason, four different point angles, which were 100°, 118°, 136°, and 154° selected. The both sides or cutting edges of drills, with 10 mm in diameter, were grinded, on a grinder machine to constitute cutting edges in different point angles. Tools were fastened to spindle of CNC machine with the help of the fastening equipment, as the clamping equipment grasped all of the shank of the drill.

The fluctuation sizes in thrust force, obtained during the drilling operations, are shown as in Fig. 2. By the help of Kistler 5233 A-model dynamometer thrust forces measured during the drilling operations. The data logger saved thrust forces values in hundreds in one-second time. Only one minimum and one maximum of these data of the fluctuation size in thrust force taken into account for per unit of a second time. Thus, the deviation in thrust force in the processes were gained from the beginning of the drilling until it was completed and drill tool started regurgitating. The fluctuation size in one-second time calculated as seen in equation 1.

$$\text{Fluctuation Size in Thrust Force}\,(\%)_{1Second}$$
$$= \frac{(F_{max} - F_{min})}{F_{max}}.100 \quad (1)$$
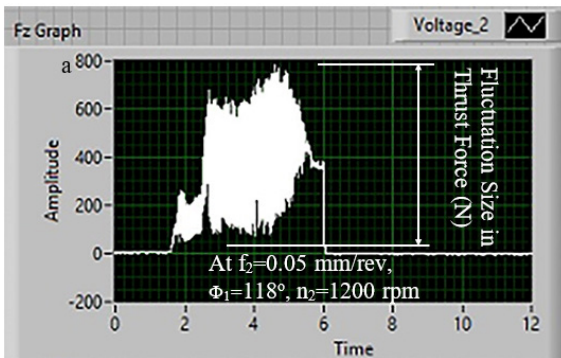
Figure 2. Fluctuation size in thrust force.

In Fig. 2 b, the chip morphology can be seen. During the drilling operation, removed chips collected for each experiment, separately. Chips morphology and chip geometrical properties were investigated by using chip photos, which were taken by using macro photo camera. Then the chips thicknesses and their widths were measured at six different positions by using digital clapper as shown in Fig. 3. The arithmetic average values of these measured data were taken into account for chip thicknesses and chip widths for each experiment separately.
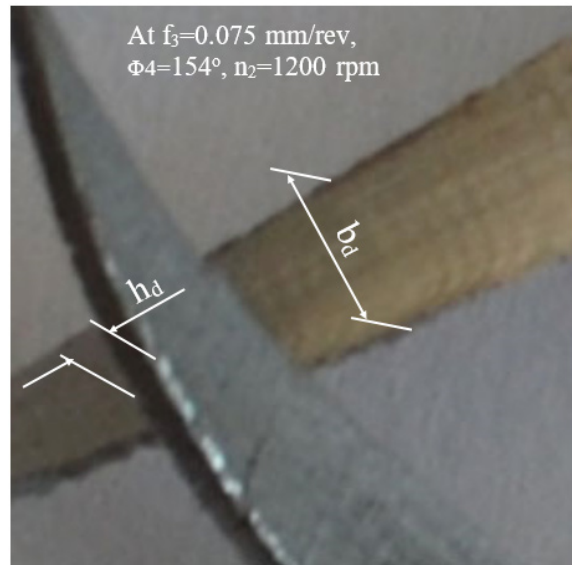
Figure 3. Chip thickness (h_d) and chip width (b_d).

THEORY OF CHIP DIMENSIONS

The shape of the tools, particularly the point angle of the drills, have an important effect on the chip geometrical dimensions, such as chip thickness and chip width in drilling operations. Because the cutting speed has an alteration on the cutting side. While at the circumference of the cutting speed takes the greatest value, these values approach zero close to the centre-line of the web of the drill, where the tool side combined to a chisel form [26]. Moreover, according to the results obtained from the experimental procedure of the present paper, with increasing point angle from 100° to 154°, thrust forces and also fluctuation in thrust forces were decreased. Even at higher spindle speeds the optimum chip shapes without deformations cracks and serration form were observed. Removed chips geometrical dimensions indicates the quality of the drilling operations, hence investigating the chip thickness and chip width consistent with the selected parameters have a major phenomenon. In Fig. 4 a and b, the shape of the tip of the drill and chip geometry can be seen. According to the chip geometry, chip geometrical dimensions, such as chip thickness and chip width can be calculated by using equations from 1 to 5, which written as at below.

If the specimens were not fore-drilled the dimension of the tool sides would be $|C_{1.1}-A_1|$, $|C_{1.2}-A_1|$, $|C_{1.3}-A_1|$, $|C_{1.4}-A_1|$ for 100°, 118°, 136°, 154° point angles, respectively. But in the present paper, we fore-drilled specimens 5 mm in diameter to exclude the effectuate of the chisel side. Consequently, the dimension of the tool side, which were used in the present paper, were $|B_1-A_1|$, $|B_2-A_1|$, $|B_3-A_1|$, $|B_4-A_1|$ for 100°, 118°, 136°, 154° point angles respectively.

In the present investigation the specimens were fore-drilled 5 mm in diameter ($\emptyset d_o$) to exclude the influence of the chisel edge. In case of the selected specimens, not pre-drilled, the un-deformed chip width namely the dimension of tool side can be computed with the help of equation 2, consistent with Fig. 5 (b). l is equal to the un-deformed chip width (b_D) of samples without pre-drilled. It had been identified with dimension of $|C_1A_1|$ as seen in Fig. 4 a.

$$l = |C_1A_1| = b_D = \frac{d_h - d_o}{2.\sin\varphi} \text{ mm} \tag{2}$$

The thickness of the un-deformed chip (h_d) can be computed relying on feed rate (f_z) and one half point angle (ϕ) as in equation 3, as demonstrated in Fig. 4 (a).

$$h_d = h_{de} = f_z.\sin\varphi \text{ mm} \tag{3}$$

As seen in Fig. 3 (a) the region of $|C_1C_{11} - A_1A_{11}|$ is representing the un-deformed chip in the operation, in which the workpieces are not fore-drilled. These can be computed relying on the dimensions of the chips (h_d and b_d), as demonstrated in Equation 4.

$$A_c = |C_1C_1^1| . |C_1A_1| = h_d.b_d \text{ mm}^2 \tag{4}$$

In the present paper, the specimens were fore-drilled 5 mm ($\emptyset d_o$) in diameter, as guiding eye. Consequently, in fore-drilling parameters the size of the tool side, in other words the width of un-deformed chip and un-deformed chip thickness are specified as (b_{de}) and (h_{de}), respectively. The effective un-deformed chip thickness is equal to the un-deformed chip thickness as shown in equal 2. But the effective un-deformed chip width is different from un-deformed chip width, because of the diameter ($\emptyset d_o$) of fore-drilled hole. It is described as in equation 5. le is equal to the effective un-deformed chip width of samples with pre-drilled holes, which is specified in Fig. 4 (a), the dimension of $|B_1A_1|$.

$$l_e = |B_1A_1| = b_{de} = \frac{d_h - d_o}{2.\sin\varphi} \text{ mm} \tag{5}$$

In the present case, the effective are of un-deformed chip (Ae) can be calculated relying on effective un-deformed chip width (b_{de}) and (h_{de}), which is shown in equation 6.

$$A_{ce} = |B_1B_1^1 - A_1A_1^1| = h_{De}.b_{De} \text{ mm}^2 \tag{6}$$

In the present paper, there are 4 dissimilar point angles ($\Phi1, \Phi2, \Phi3, \Phi4$) are expressed in the Fig. 4 (b), which were selected in experimental study, as 100°, 118°, 136°, 154° respectively. Consistent with the form of tool point, the alteration of cutting side dimension (l) and (l_e), in other words un-deformed chip widths (b_d) and (b_{de}), are replaced with different of point angles.

The zone of un-deformed chip in the processes, considerably depend on the tool side dimension, in other words un-deformed chip wideness. Consistent with the equations 2, 4, and 5, the effectual un-deformed chip height (h_d), the tool side dimension (l_e) in other words un-deformed chip width (b_d), and accordingly, un-deformed chip area (A_{ce}) can compute in compliance with feed rate and point angle. Relying on the form of the tip of the tool, as mentioned at above, the un-deformed chip height is only associated with both one cutting edge feed rate (f_z) at per rotation and point angle. The drill side dimension in other words un-deformed chip width is depending on diameter and point angle of the drill. Hence forth, every both one feed rate and one-point angle
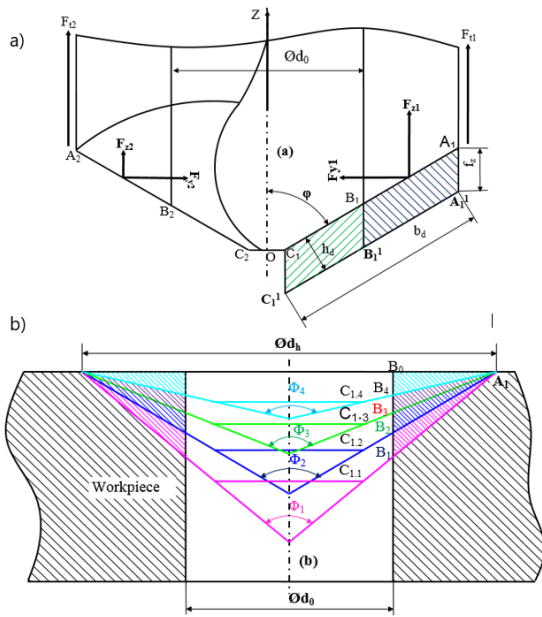
Figure 4. (a) The front view of the tip of the drill, chip thickness and chip width (b) removal chip area consistent with the point angle and pre-drilled hole geometry.

Table 2. Computed un-deformed chip dimension are consistent with feed rate and point angle, demonstrated with icon.

Icon	Feed Rate	Point Angle	$h_{de}=h_d$	b_d namely l_e	$Ace=h_{de}*b_{de}$
A	f_{z1}=0.025 mm/rev		0.0161 mm		0.0525 mm²
B	f_{z2}=0.050 mm/rev	$\Phi1$=100°	0.0321 mm	3,2635 mm	0.1048 mm²
C	f_{z3}=0.075 mm/rev		0.0482 mm		0.1573 mm²
D	f_{z1}=0.025 mm/rev		0.0129 mm		0.0376 mm²
E	f_{z2}=0.050 mm/rev	$\Phi2$=118°	0.0258 mm	2,9166 mm	0,0753 mm²
F	f_{z3}=0.075 mm/rev		0.0386 mm		0,1126 mm²
G	f_{z1}=0.025 mm/rev		0.0094 mm		0,0254 mm²
H	f_{z2}=0.050 mm/rev	$\Phi3$=136°	0.0187 mm	2,6963 mm	0,0504 mm²
I	f_{z3}=0.075 mm/rev		0.0281mm		0,0758 mm²
J	f_{z1}=0.025 mm/rev		0.0056 mm		0,0144 mm²
K	f_{z2}=0.050 mm/rev	$\Phi4$=154°	0.0112 mm	2,5658 mm	0,0287 mm²
L	f_{z3}=0.075 mm/rev		0.0169 mm		0,0434 mm²
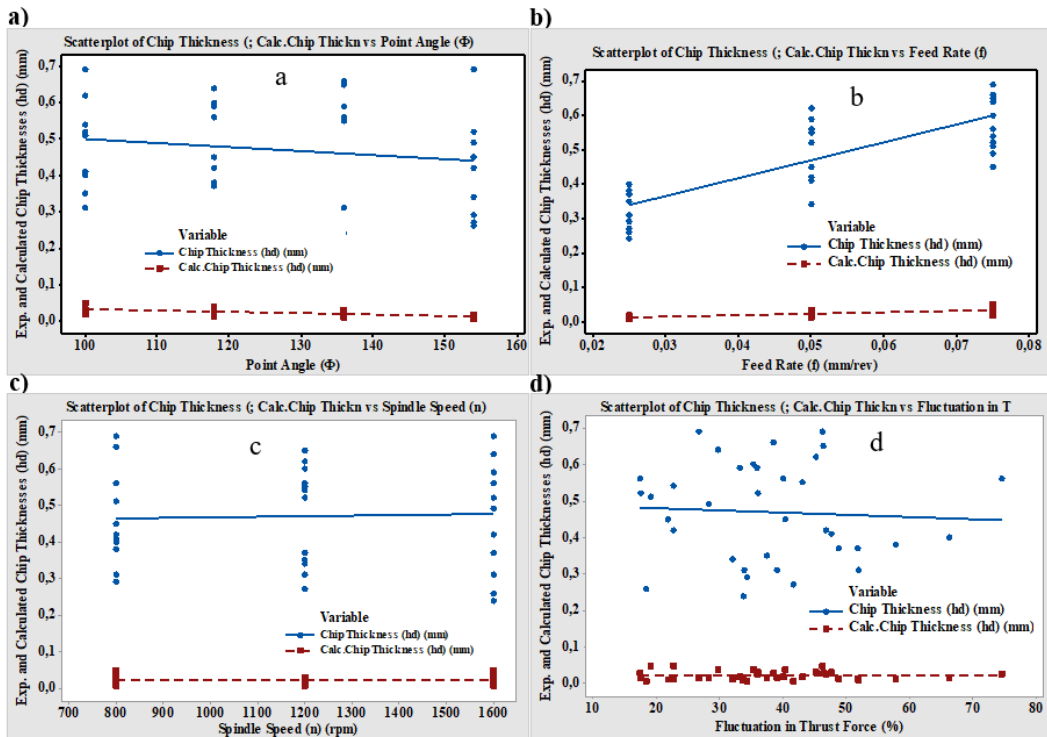
Figure 5. The effect of (a) point angle (b) feed rate, (c) spindle speed, (d) fluctuation in thrust force on experimental and calculated chip thicknesses.

conditions pairs are demonstrated with icons: A, B, C, D, E, F, G, H, I, J, K, and L, as seen in Table 2. The effective undeformed chip area (A_{ce}), in Table 2, was calculated according to equation 5.

Chip geometrical dimensions demonstrate the quality of the drilling. Especially, the chip thickness ratio, which can be identified proportion of distorted chip thickness to the un-distorted chip thickness, is a major geometrical characteristic, which demonstrates the quality of the process. This quality is evaluable according to the chip thickness ratio. When chip thickness ratio is bigger than 60 not available, between 60-30 confined available, chip thickness ratio is between 30-11, it is available, and when chip thickness ratio is between 10-3 is the best. Additionally, the chip thickness ratio is smaller than 3 is good in machining operations, which is demanding ratio with regard to the quality of the process [27]. In this study, chip morphology was investigated according to the chip geometrical dimensions, especially chip thickness ratio.

RESULTS AND DISCUSSION

Chip Geometrical Dimensions and Fluctuation Size in Thrust Force

Due to they are important dimensions, the chip geometrical dimensions, such as chip thickness, chip width and chip morphology indicates the quality of the drilling ope-

ration. In this study, the theoretical chip thickness and chip width calculated using equations 2 and 4 consistent with the feed rate for per tool side (f_z) and point angle. Experimental chip thickness and chip width dimensions were measured by using digital clapper as seen in Fig. 3. Therefore, the calculated and experimental chip thickness and width values were compared.

In Fig. 5 a, b, c, and d, the influence of point angle, feed rate, spindle speed, and fluctuation size in thrust force on both experimental and calculated chip thicknesses values can be shown, respectively. According to these graphs, the most influential parameter on chip thicknesses was feed rate, which followed by point angle, fluctuation size in thrust force and spindle speed, respectively. The experimental chip thickness values were greater than the calculated values. Moreover, with increasing point angle and fluctuation in thrust force experimental chip thickness values were little decreased, but it was increased linearly with increasing feed rate. However, spindle speed did not affect neither experimental nor calculated chip thickness values. Moreover, this consequence verifies the accuracy of the equations 4, 5, and 6.

The effect of point angle on the experimental chip thickness was smaller than calculated chip thickness, due to motions and deformations effect in drilling operations. Calculated chip thickness was decreased linearly by increasing point angle from 100° to 154°. Chip thicknesses values were
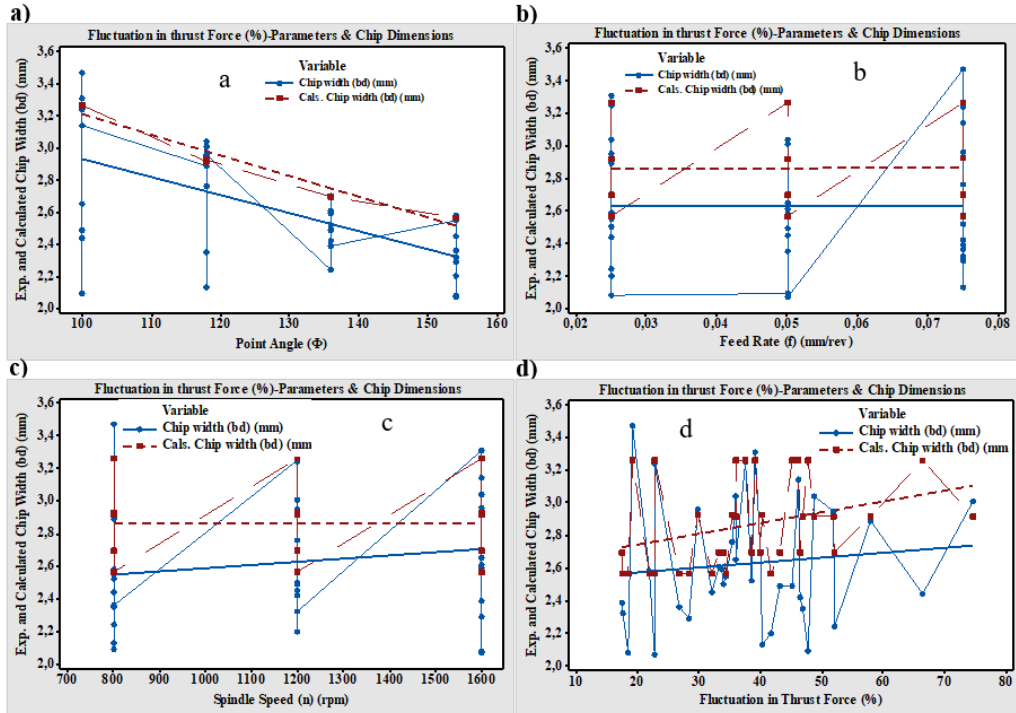
Figure 6. The effect of (a) point angle, (b) feed rate, (c) spindle speed, (d) fluctuation in thrust force on experimental and calculated chip widths.

not change with changing spindle speed, while there was a little variation in chip thicknesses values with changing fluctuation size in thrust force. However, both experimental and calculated chip thicknesses values were increased linearly with increasing feed rate. Calculated chip thickness shown an increase with increasing feed rate according to equation 2. In equation 2, un-deformed chip thickness relies on only the feed rate and point angle of per cutting edge in one revolution.

Like chip thickness, chip width dimension effects the removal chip volume in drilling operations. The effects of the parameters, namely point angle, feed rate, spindles speed, and fluctuation size in thrust force are shown in Fig. 6 a, b, c, and d, respectively. Consistent with the equation 4, feed rate and spindle speed did not have any effect on calculated chip width, while they had a little effect on experimental chip width, due to the motion and thrust effects of the drill. According to the equation 4, the calculated chip width decreased regularly with increasing point angle from 100o to 154o. In comparison with chip thickness, the chip width decreased linearly with increasing point angle. This outcome indicates that chip width is a parameter, depending on point angle of drill, in drilling operations. Both experimental and theoretical chip widths values graphs shown a collateral variation. Fluctuation size in thrust force effected the calculated chip width values more than the experimental values. With increasing fluctuation size in thrust force, chip width values were increased linearly.

Main effect of parameters on both calculated and ex-

perimental chip thicknesses and chip thick ratio can be demonstrated as in Fig. 7 a, b, and c, respectively. According to these graphs, both calculated and experimental chip thickness values were regularly increased with increasing feed rate, but calculated chip thickness decreased. At point angles bigger than 136o experimental chip thickness linearly decreased. Spindle speed had not any effect on calculated chip thickness. However, experimental chip thickness values were shown a little changing in the direction of increase, due to the motion and thrust effects during drilling.

The most influential parameter on chip thickness ratio was feed rate. Therefore, at higher selected feed rates chip thickness was regularly decreased, but with increasing point angle chip thickness ratio was increased. Although this result is not demanded in machining operations they are not poor, due to the differences between calculated and experimental chip thickness values, according to the point angle. Calculated chip thickness values were small according to equation 2, but experimental chip thickness values were enormous. Thus, the ratio of these values naturally resulted in high values. Chip width is a dimensional result in machining operations, affecting the volume of the removal chip. According to the equation 4, the most influential parameter on chip width is point angle. Therefore, increasing in point angle provided to decrease in calculated chip width, as seen in Fig. 7 d. However, calculated chip width is not shown any variation with changing both spindle speed and feed rate. While the variation in both experimental and calculated chip widths shown a collateral decreasing with increasing
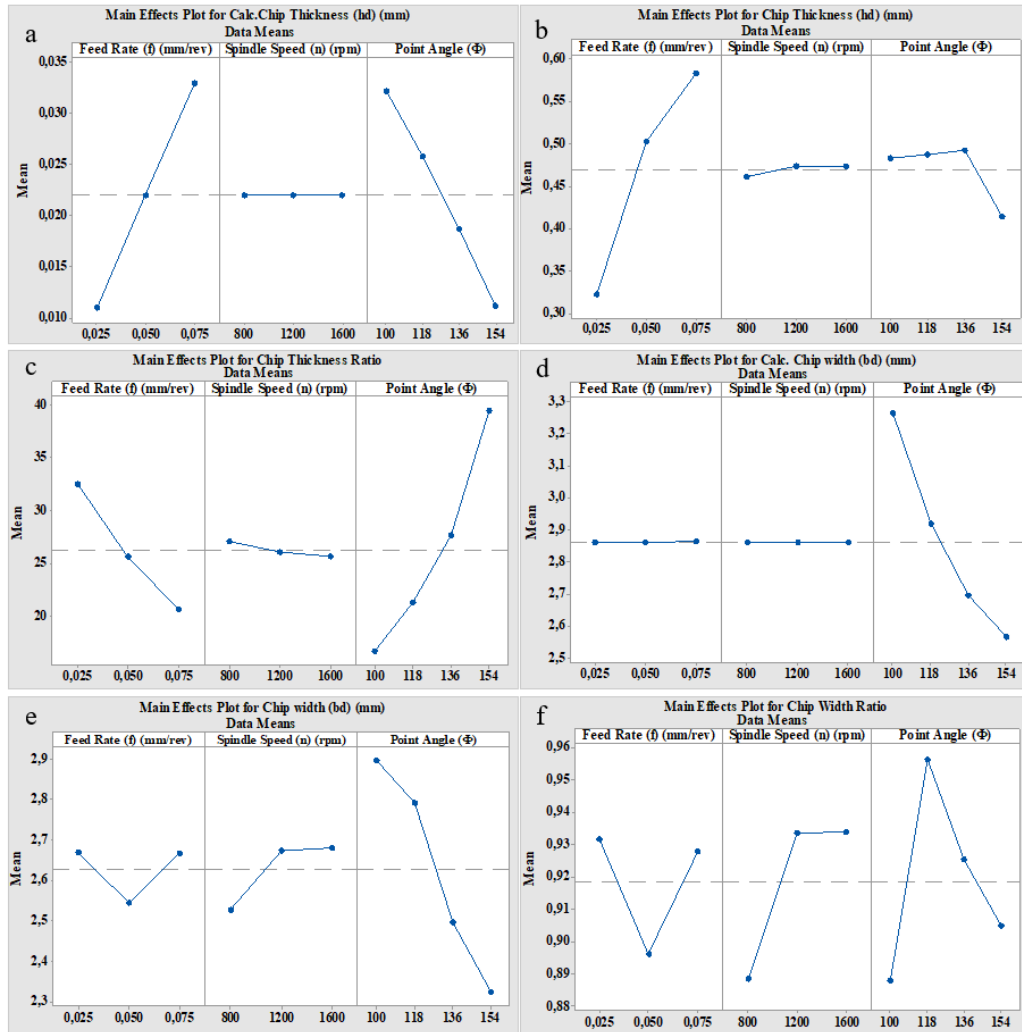
Figure 7. Main effect of parameters on (a) calculated chip thickness (b) experimental chip thickness (c) chip thickness ratio (d) calculated chip width (e) experimental chip width (f) chip width ratio.

point angle, there was a little changing only in experimental chip width values with increasing both spindle speed and feed rate, as observed in Fig. 7 e.

Chip thickness ratio was got its peak value at point angles between 100° and 118°, but then it was decreased regularly with increasing point angle to 154°. It was reduced at smaller feed rates, but it was increased at higher selected spindle speeds. However, this variation in chip thickness ratio consistent with both feed rate and spindle speed was shown an irregular changing, as seen in Fig. 7 f.

Chip Morphology

Chip thickness ratio is a major result in machining operations, identifying the quality of the process according to the morphology of removed chips. The most demanded chip ratio values in the machining operations are between 3-10. When the removal chip thickness ratio is in

these limits, it shows that the machining operation carried out in the most appropriate conditions. Additionally, continuous, ductile, and longer form chips indicate better machining conditions. The effect of chip thickness ratio, chip width ratio and fluctuation size in thrust force on chip morphology can be seen in Fig. 8 a, at 0,025 mm/rev, in Fig. 8 b, at 0,050 mm/rev, and in Fig. 8 c, at 0,075 mm/rev feed rates.

At 0,025 mm/rev feed rate, chip morphology showed variations depend on chip thickness ratio, chip width ratio, and fluctuation size in thrust force, from brittle, shorter chip forms to continuous, ductile, and longer. Even at lower chip thickness ratios and fluctuation in thrust forces, the chips removed in the form of brittle and shorter forms, at 100° and 118°, but at 136° and 154° point angles, even at higher chip thickness ratio, chip width ratio, and fluctuation size in thrust force values, removed chips were in long, continuous and ductile forms, which indicate better results. However,
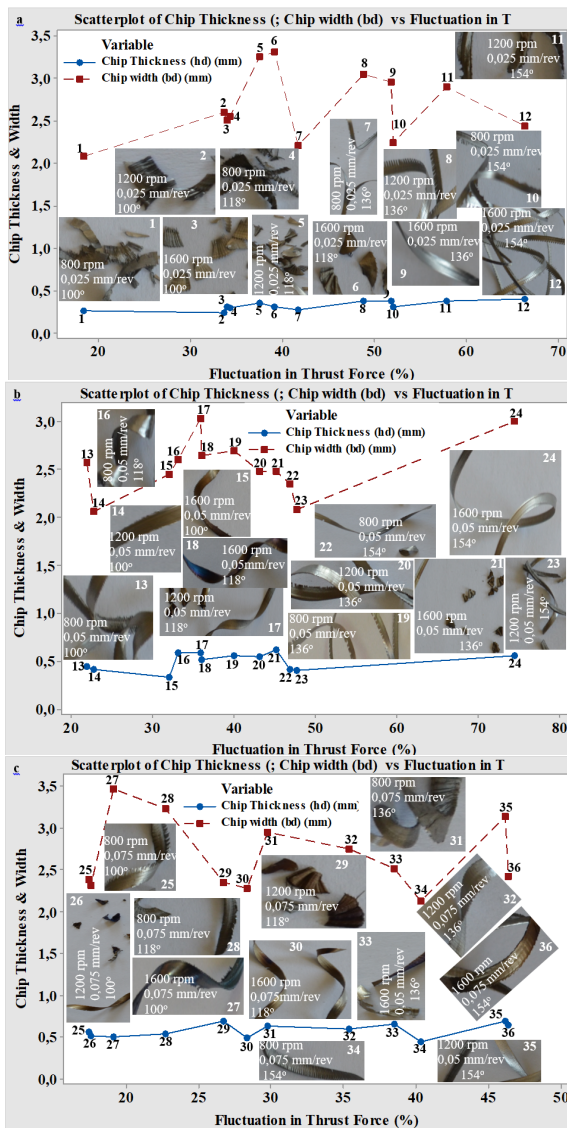
Figure 8. Chip morphology according to chip thickness ratio, chip width ratio, and fluctuation size in thrust force, (a) at 0,025 mm/rev, (b) at 0,050 mm/rev, (c) at 0,075 mm/rev feed rates.

there were deformation traces and cracks on the chip morphology at 0,025 mm/rev feed rate. Additionally, the lower fluctuation in thrust force (%) recorded at 154° point angle and chip thickness ratio values were bigger than 21.

The least chip thickness values were recorded as 12,77 μm and 10,58 μm at 100° point angle, at both 0,050 and 0,075 mm/rev feed rates, respectively. But there were deformation cracks and traces on removed chip shapes collective with burning marks at higher spindle speeds. At 0,050 mm/rev feed rate, both chip thickness and chip width ratios were decreased at higher point angles. Although there was higher fluctuation size in thrust force at higher point angles, chip thickness and chip width ratios were decreased and removed chips were obtained in the continuous, ductile, and longer forms.

At 0.075 mm/rev feed rate, the effect of thrusting causes to deteriorate the deformed chip morphology as deformation traces and cracks on the chips. Beside, at higher spindle speed, there were burning marks in the black colour on the deformed chips, at all selected the remain parameters. At 0,050 mm/rev feed rate and 1600 rpm spindle speed conditions, the removed chip form can be shown as an example for this phenomenon, as seen in Fig. 8 c.

According to the chip thickness and chip width ratios criterion, also fluctuation size in thrust force, 100° and 118° point angles were appropriated parameters. However, according to the chip morphology criterion, 136° and 154° point angles were more appropriate parameters. In addition to all achieved results, namely chip thickness, chip width, chip thickness ratio, chip width ratio, and fluctuation size in thrust force, the most appropriate parameters were 0,025 mm/rev feed rate - 800 rpm spindle speed, 0,050 mm/rev feed rate- 1200 rpm spindle speed, and 0,075 mm/rev feed rate – 1600 rpm spindle speed couples.

CONCLUSION

Chip morphology and especially distorted chip sizes like chip thickness, chip width, chip width and chip thickness ratios, affect the results in machining operations. Continuous, ductile, and longer chip forms, which demanded deformed chip forms, while brittle and shorter chip forms, which were undesired in machining operations.

The most influential parameters on both theoretical and experimental chip thicknesses were feed rate and point angle, while little influential parameters only on experimental chip thickness were spindle speed and fluctuation size in thrust force.

Chip thickness ratio was bigger than 10, while chip width ratio smaller than 1,1. This indicated that chip thickness ratio was more changeable dimensional parameter than chip width and it was the most influential dimensional result, which affects the quality of the machining operations.

The most influential parameters on chip thickness were feed rate, followed by point angle. However, the most influential parameter on chip width was only point angle. Therefore, point angle was a vital parameter, affecting the chip morphology and chip dimensional geometries in drilling operations.

Decreasing in point angle provided appropriate chip morphology in drilling operations, even at higher fluctuations in thrust force and chip thickness ratio. While at lower point angles the brittle and shorter chip morphology were obtained, at higher point angles continuous, ductile, and

longer chip forms were obtained. The most appropriate chip morphology was resulted in at lower feed rate, higher spindle speed and point angles. However, at higher spindle speeds there were burning marks on the removed chips in black colour. Additionally, even at higher spindle speed and point angles, the most demanded chip morphology was achieved.

According to chip thickness ratio and chip morphology criterion, the most appropriate parameters couples were 800 rpm-0,025 mm/rev, 1200 rpm-0,050 mm/rev, and 1600 rpm-0,075 mm/rev spindle speeds and feed rates, respectively.

The lower chip thickness ratio values were recorded at 100° and 118° point angles, at 0,025 mm/rev feed rate and 800 rpm spindles speed. However, the obtained deformed chips were in brittle and shorter forms.

References

1. Thakre, A. A. and Soni, S. (2016) Modelling of bur size in drilling of aluminium silicon carbide composites using response surface methodology, Eng. Sci. Technol. Int. j., http://dx.doi.org/10.1016/j.jetch.2016.02.007.

2. Chen, W. C. and Tsao, C. C. (1999) Cutting performance of different coated twist drills, J. Mater. Process. Technol. 88, 203 – 207.

3. Lazar, M. B. and Xiraouchhakis, P. (2013) Mechanical load distribution along the main cutting edges in drilling, J. Mater. Process. Technol., 213, 245 – 260.

4. Kalidas, S. Devor, R. E. Kapoor, S. G. (2001) Experimental investigation of the effect of drilling coatings on hole quality under dry and wet drilling conditions. Surf. Coat. Technol., 148, 117 – 128.

5. Taskesen, A. Kütükde, K. Biermann, D. (2013) Experimental investigation and multi-objective analysis on drilling of boron carbide reinforced metal matrix composites using grey relational analysis, Measurement, 47, 321-330.

6. Celik, Y. H. (2014) Investigation the effect of cutting parameters on the hole quality in drilling the Ti-6Al-4V. Mater. Technol., 95, 669-295.

7. Caydas, U. and Celik, M. (2017) Investigation of the effects of cutting parameters on the surface roughness, tool temperature and thrust force in drilling of AA 7075-T651 alloy, J. Polytech., 20(2), 419–425.

8. Caydas, U. Hascalık, A. Buytoz, O. Meyveci, B. (2011) Performance evaluation of different twist drills in dry drilling of AISI 304 austenitic stainless steel, Mater. Manuf. Process., 26, 951-960.

9. Palanikumar, K. and Muniaraj, A. (2014) Experimental investigation and analysis of thrust force in drilling cast hybrid metal matrix (Al-15%SiC-4%graphite) composite, Measurement, 53, 240–250.

10. Sultan, A. Z. Sharif, S. Kurniawan, D. (2015) Chip formation when drilling AISI 316L stainless steel using carbide twist drill, Procedia Manufacturing, 2nd Int. Mater. Ind. Manuf. Eng. Con., MIMEC2015 4-6 February 2015, Bali Indonesia, 2, 224-229.

11. Samy, G. S. and Kumaran, S. T. (2017) Measurement and analysis of temperature, thrust force and surface roughness in drilling of AA (6351)-B4C composite, Measurement, 103, 1–9.

12. Thamizhmanii, S. and Hasan, S. (2012) Machinability study using chip thickness ratio on difficult to cut metals by CBN cutting tool, Key Eng. Mater., 504-506, 1317–1322.

13. Celik, Y. H. Yildiz, H. Ozek, C. (2006) Effect of cutting parameters on workpiece and tool properties during drilling of Ti-Al-4V, Wear Test., 46, 1526–1535.

14. Ema, S. (2012) Effect of twist drill point geometry on torque and thrust. Sci. Rep. Fac. Educ. Gifu Univ. (Nat. Sci.) 36, 165-174.

15. Ramesh, B. Elayaperumal, A. Satishkumar, S. (2014) Effect of the standard and special geometry design of a drill body on quality characteristics and multiple performance optimization in drilling of thick laminated composites, Procedia Eng., 12th Global Con. Manuf. Manage., GCMM 2014 97, 390-401.

16. Wang, J. Feng, P. Zheng, J. Zhang, J. (2016) Improving hole exit quality in rotary ultrasonic machining of ceramic matrix composites using a compound step-taper drill, Ceram. Int., 42, 13387-13394.

17. Paul, A. Kapoor, S. G. DeVor, R. E. (2005) Chisel edge and cutting lip shape optimization for improved twist drill point design, Int. J. Mach. Tools Manuf., 45, 421-431.

18. Sui, J. Kountanya, R. Guo, C. (2016) Development of a mechanistic force model for CNC drilling process simulation, Procedia Manuf., 44th Proceedings of the North America Manuf. Research Inst. SME, 5, 787–797.

19. Tsao, C. C. and Hocheng, H. (2003) The effect of chisel length and associated pilot hole on delamination when drilling composite materials, Int. J. Mach. Tools Manuf., 43, 1087-1092.

20. Ghosh, R. Sarkar, R. Paul, S. Pal, S. K. (2016) Biocompatibility and drilling performance of beta tricalcium phosphate: Yttrium phosphate bioceramic composite, Ceram. Int., 42, 8263-8273.

21. Ahmadi, K. and Savilov, A. (2015) Modeling the mechanics and dynamics of arbitrary edge drills, Int. J. Mach. Tools Manuf., 89, 208-220.

22. Saoudi, J. Zitoune, R. Mezlini, S. Gururaja, S. Seitier, P. (2016) Critical thrust force predictions during drilling: Analytical modeling and X-ray tomography quantification, Comp. Str., 153, 886–894.

23. Anand, S. R. and Patra, K. (2017) Mechanistic cutting force modelling for micro-drilling of CFRP composite laminates, CIRP J. Manuf. Sci. Technol., 16, 55–63.

24. Karimi, N. Z. Heidary, H. Minak, G. (2016) Critical thrust and feed prediction models in drilling of composite laminates, Comp. Str., 148, 19-26.

25. Jia, Z. Fu, R. Niu, B. Qian, B. Bai, Y. Wang, F. (2016) Novel drill structure for damage reduction in drilling CFRP composites. Int. J. Mach. Tools Manuf., 110, 55–65.

26. Akkurt, M. (1996) Talaş kaldırma yöntemleri ve takım tezgahları, 3rd, Birsen Press, İstanbul.

27. Rey, R. A. LeDref, J. Senatore, J. Landon, Y. (2016) Modelling of cutting forces in orbital drilling of titanium alloy Ti-6Al-4V, Int. J. Mach. Tools Manuf., 106, 75–88.